

## 1. Summary

- A high-resolution 25-year simulation is performed in Gulf Stream (GS) region using a coupled physical-biological model.
- A large sample of mesoscale eddies are detected and tracked, and the eddy-centric composites are created.
- The long-term averaged contribution of cyclonic eddies (CEs) and anticyclonic eddies (ACEs) to the vertical  $\text{NO}_3$  flux into the euphotic zone ( $Z_{\text{eu}}$ ) are both positive.
- The eddy-wind-interaction-induced Ekman pumping is likely the dominant mechanism for the enhanced  $\text{NO}_3$  flux at  $Z_{\text{eu}}$  in ACEs.

## 2. Numerical Model

- Physical model: ROMS over Northwest Atlantic (NWA) with 7km horizontal resolution and 40 vertical levels
- Biogeochemical model: NOAA/GFDL's Carbon, Ocean, Biogeochemistry and Lower Trophics (COBALT) model

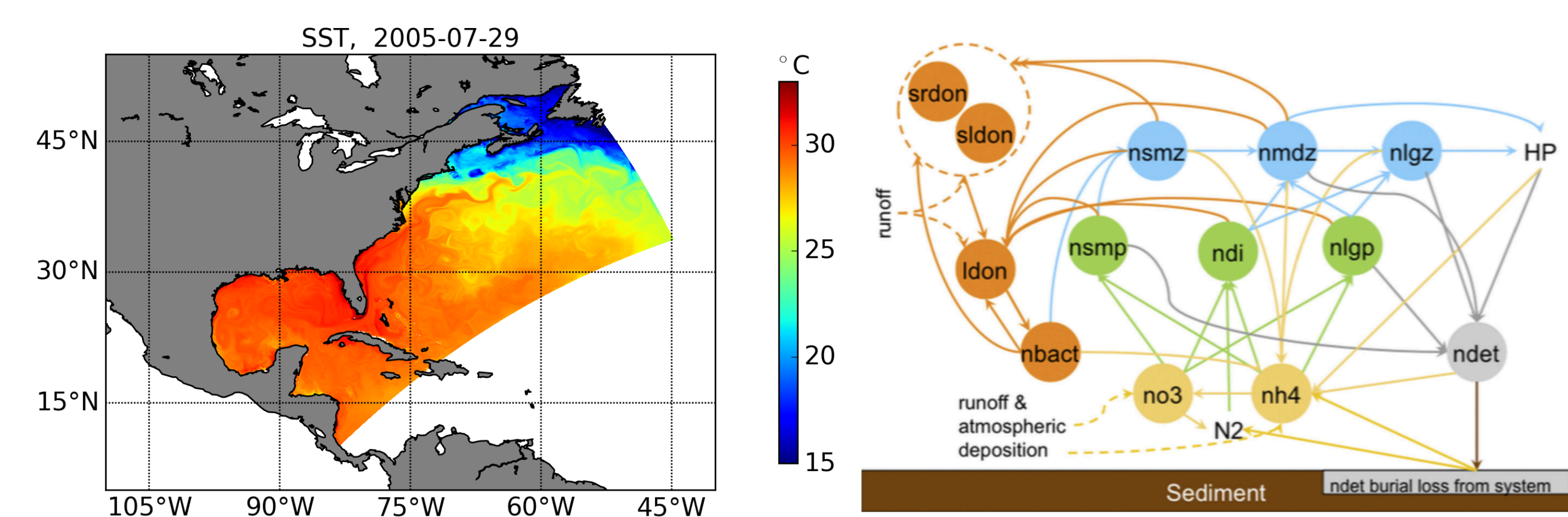


Fig 1. (Left) A snapshot of SST from ROMS-COBALT simulation. (Right) Schematic of N-based state variables in COBALT [Stock et al., 2014b].

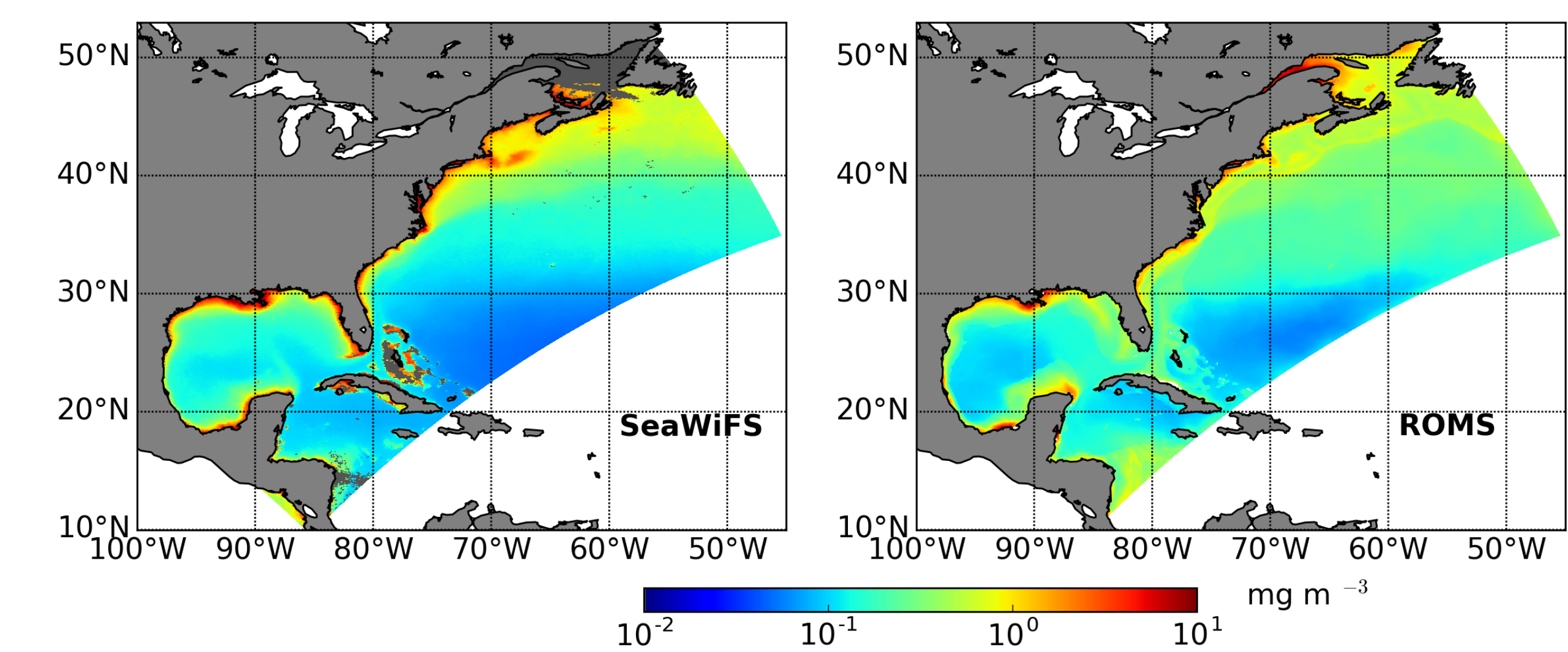


Fig 2. Mean surface chl from (left) SeaWiFS during 1998-2007 and (right) coupled ROMS-COBALT simulation during 1983-2007.

## 3. Eddy Detection and Tracking

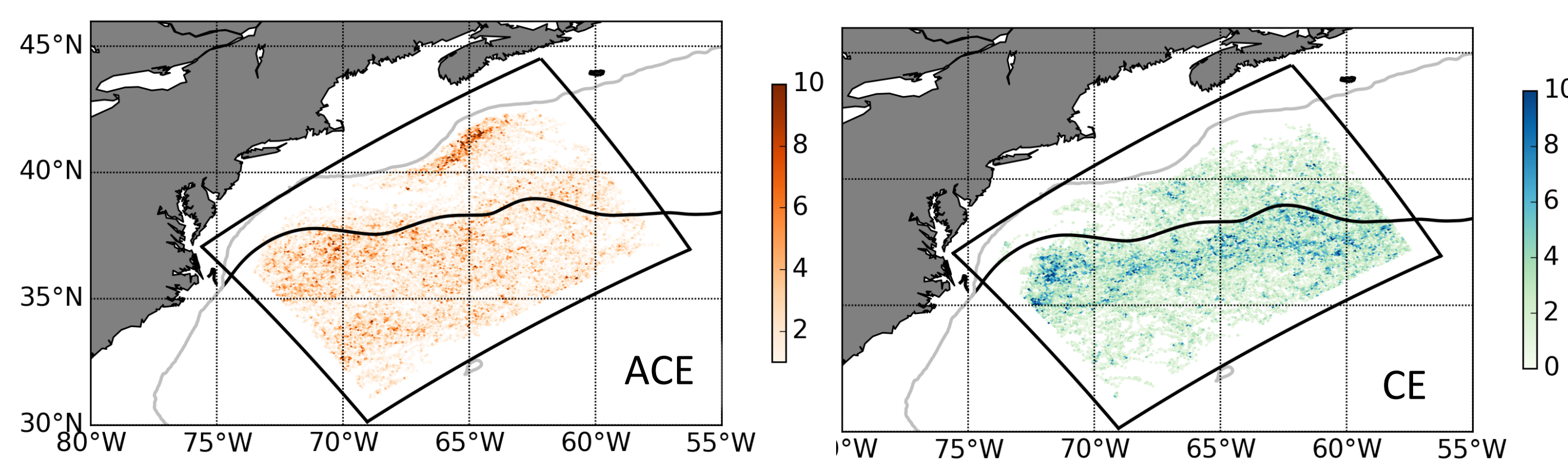


Fig 3. ACE and CE occurrence during 1983-2007. Black curve is the mean GS pathway and grey contour is the 1000m isobath.

Table 1. Eddy properties with standard deviations in parentheses.

	Number		Duration (days)	Radius (km)	Distance (km)
	Total	Per year			
ACE	740	30 (5.5)	31 (7.5)	81 (27.7)	167 (39.6)
CE	612	24 (5.3)	46 (20.63)	88 (21.2)	193 (72.1)

## 4. Eddy Composites

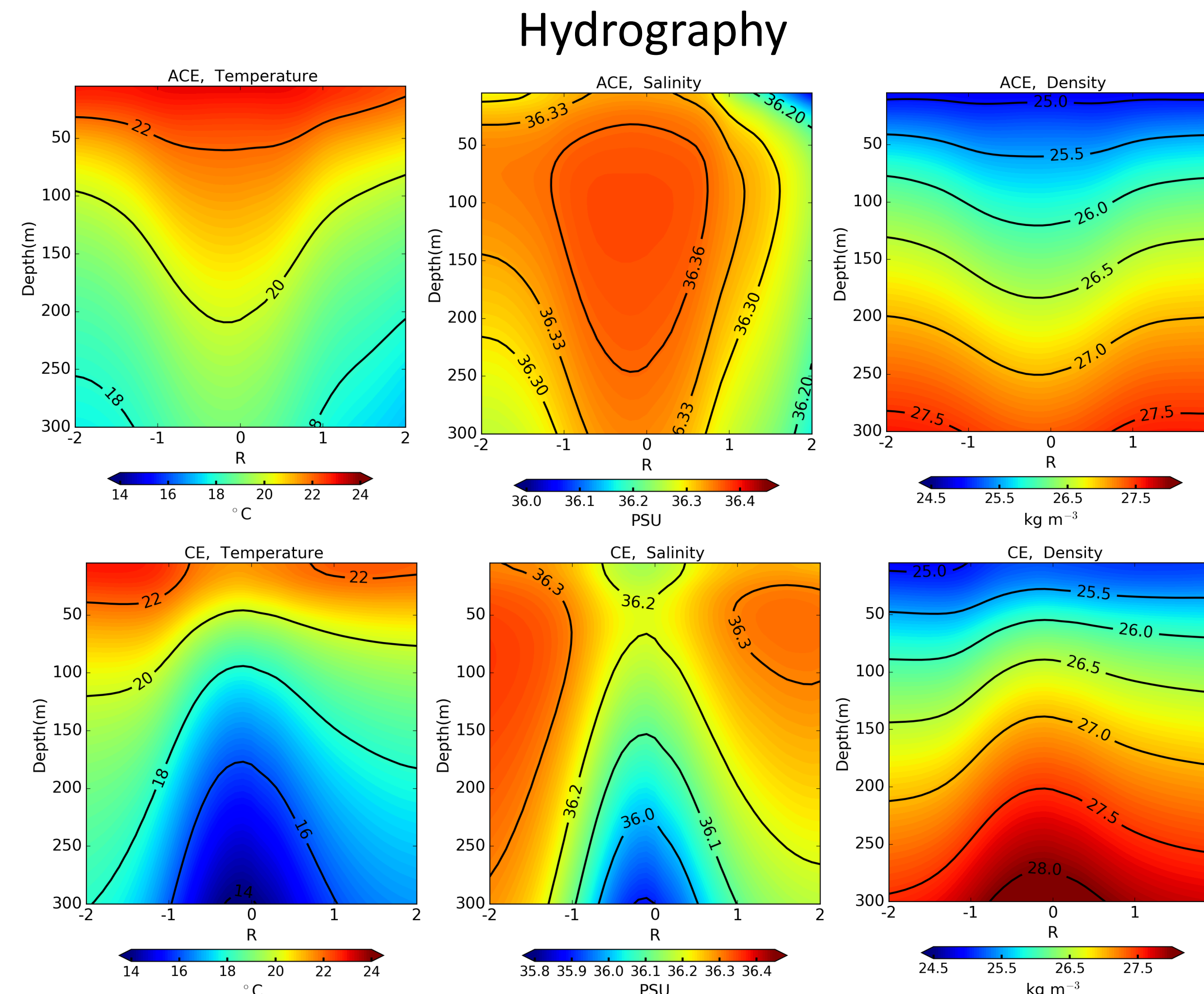


Fig 4. Composites of temperature, salinity and potential density in (upper) ACE and (lower) CE along the vertical-latitude transect across the eddy center. x-axis is the normalized radius; negative (positive) means south (north).

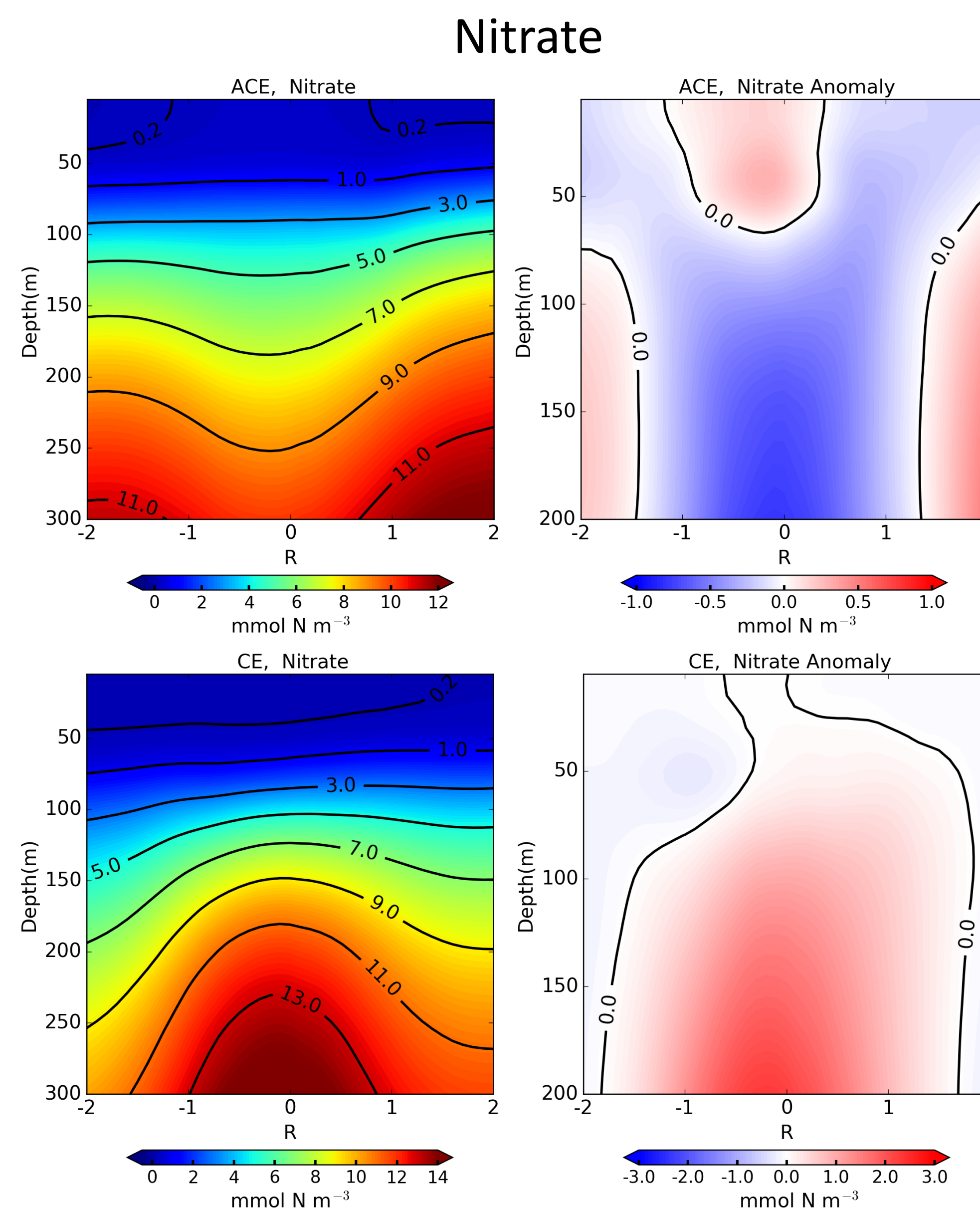


Fig 5. Composites of  $\text{NO}_3$  and its anomalies for (upper) ACE and (lower) CE.  $\text{NO}_3$  anomalies are derived by subtracting the annual average from the daily field.

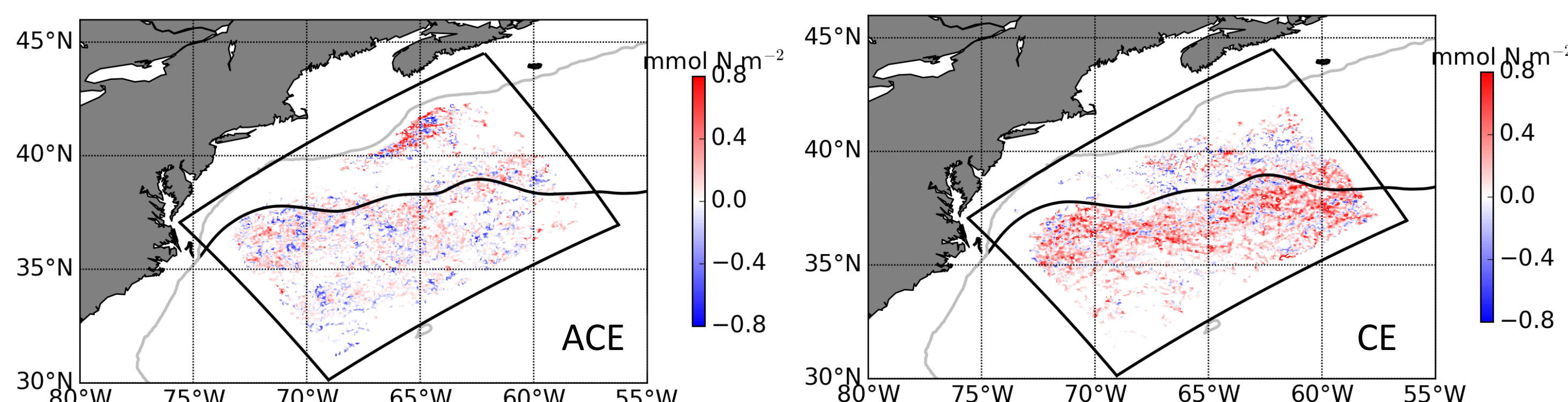


Fig 6. Vertical-integrated  $\text{NO}_3$  anomalies for all (left) ACEs and (right) CE above  $Z_{\text{eu}}$ .

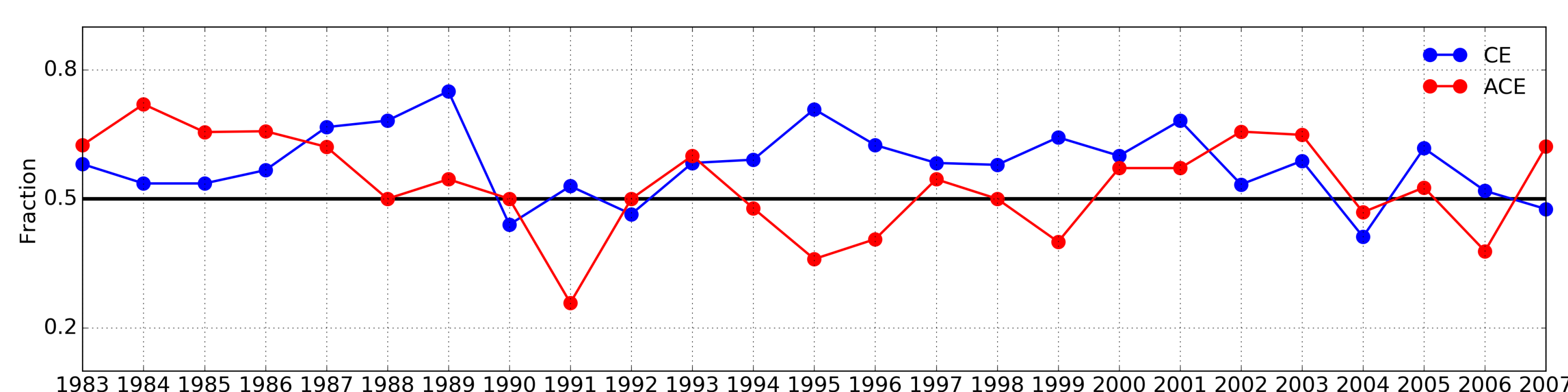


Fig 7. Fraction of ACEs (red) and CE (blue) with positive  $\text{NO}_3$  anomalies above  $Z_{\text{eu}}$ .

## 5. Mechanism

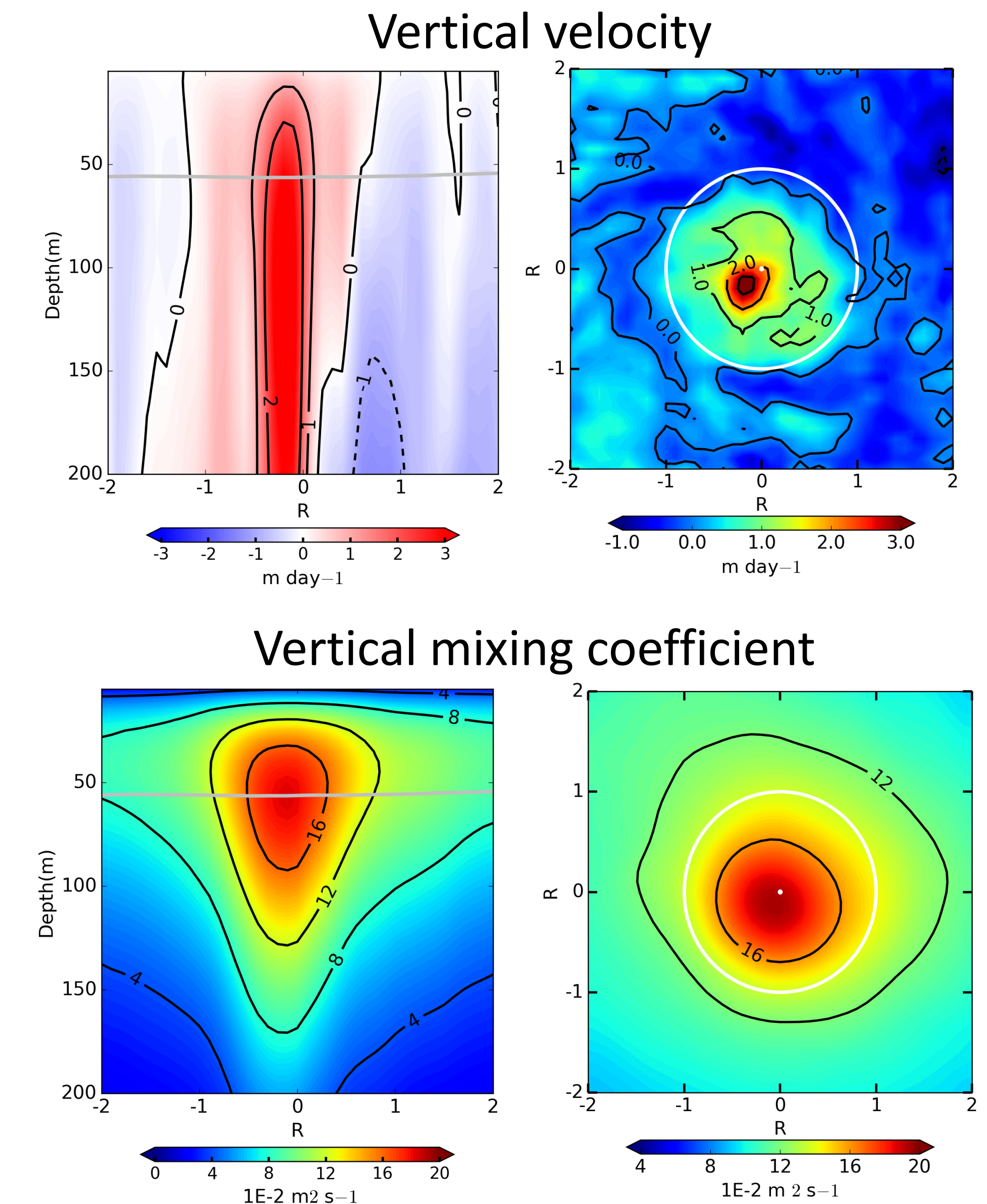


Fig 8. Composites of vertical velocity and mixing coefficient (left) along the latitudinal transect across the eddy center and (right) on the horizontal plan  $Z_{\text{eu}}$  in ACE.

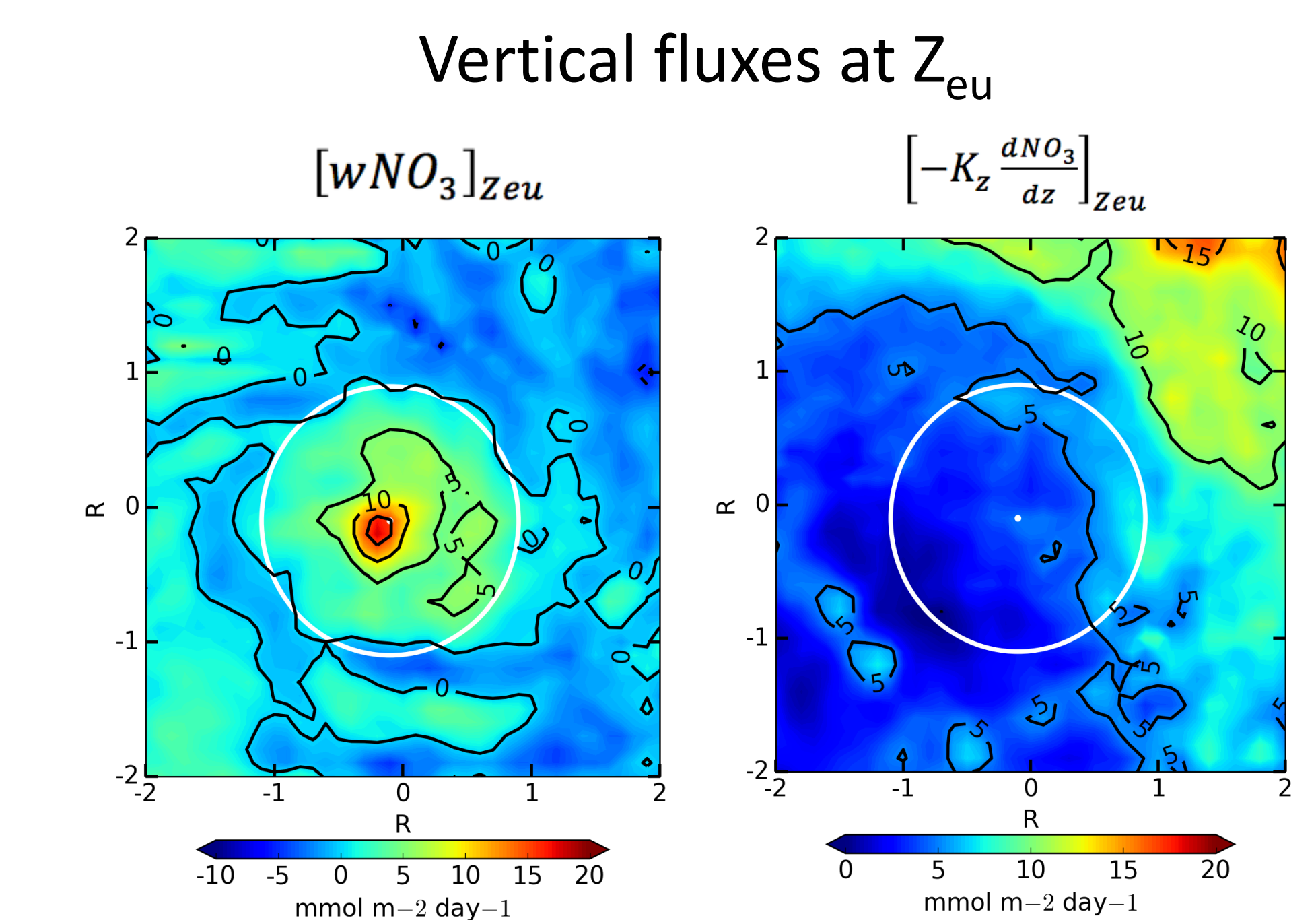


Fig 9. Vertical  $\text{NO}_3$  flux driven by (left) vertical advection and (right) vertical mixing at  $Z_{\text{eu}}$  in ACE.

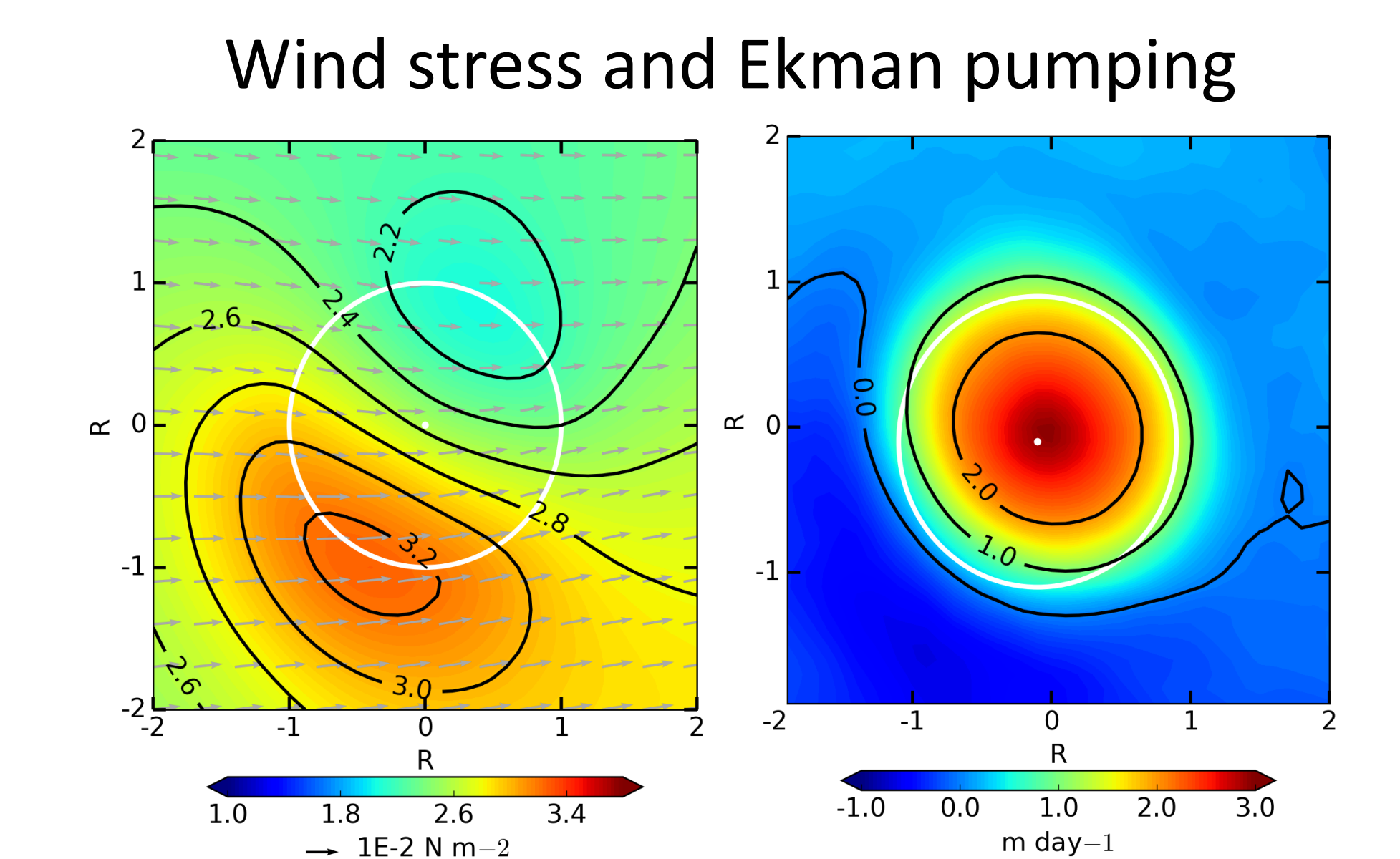


Fig 10. (Upper) Wind stress over ACE and the Ekman pumping velocity  $w_e$ . (Left) Schematic of the wind-current-interaction-induced Ekman pumping.

## 6. Reference

- Stock, C.A., J.P. Dunne, and J.G. John (2014b), Global-scale carbon and energy flows through the marine planktonic food web: an analysis with a coupled physical-biological model, *Prog Oceanogr.*, 120, 1-28.
- Kang, D., and E. N. Curchitser (2013), Gulf Stream eddy characteristics in a high-resolution ocean model, *J. Geophys. Res. Oceans*, 118, 4474-4487
- McGillicuddy, D., et al. (2007), Eddy/wind interactions stimulate extraordinary mid-ocean plankton blooms, *Science*, 316(5827), 1021.